

Ferronickel enrichment by fine particle reduction and magnetic separation from nickel laterite ore

Xiao-hui Tang¹⁾, Run-zao Liu¹⁾, Li Yao^{1,2)}, Zhi-jun Ji¹⁾, Yan-ting Zhang^{1,3)}, and Shi-qi Li¹⁾

1) School of Metallurgical and Ecological Engineering, University of Science and Technology, Beijing 100083, China

2) Hebei Iron and Steel Co. Ltd., Tangshan Branch, Tangshan 063020, China

3) Tianjin Pipe Group Co. Ltd., Tianjin 300301, China

(Received: 28 March 2014; revised: 14 May 2014; accepted: 20 May 2014)

Abstract: Ferronickel enrichment and extraction from nickel laterite ore were studied through reduction and magnetic separation. Reduction experiments were performed using hydrogen and carbon monoxide as reductants at different temperatures (700–1000°C). Magnetic separation of the reduced products was conducted using a SLon-100 cycle pulsating magnetic separator (1.2 T). Composition analysis indicates that the nickel laterite ore contains a total iron content of 22.50wt% and a total nickel content of 1.91wt%. Its mineral composition mainly consists of serpentine, hortonolite, and goethite. During the reduction process, the grade of nickel and iron in the products increases with increasing reduction temperature. Although a higher temperature is more favorable for reduction, the temperature exceeding 1000°C results in sintering of the products, preventing magnetic separation. After magnetic separation, the maximum total nickel and iron concentrations are 5.43wt% and 56.86wt%, and the corresponding recovery rates are 84.38% and 53.76%, respectively.

Keywords: laterites; ore reduction; magnetic separation; thermodynamics; fine particle metallurgy

1. Introduction

According to the survey report of the United States Geological Survey (USGS), approximately 60% of nickel resources in the Earth's crust are in the form of nickel laterite ore, and the rest belongs to nickel-bearing sulfide ore [1]. More than 60% of the world's nickel production, however, comes from nickel sulfide ore [2–4]. With the continuous exploitation of high-grade nickel sulfide ore, the development of nickel laterite ore will be the main direction of the nickel industry in the future [5]. Nickel sulfide ore forms nickel laterite ore in tropical or subtropical environments through long-term weathering, leaching, and sedimentation. It is a hydrous and porous clay oxide mineral made up of iron, magnesium, and silicon; the ore is red in color due to iron oxidation [6–7].

Currently, nickel laterite ore is difficult to concentrate due to its low nickel content and the isomorphic goethite or serpentine crystalline structure; thus, pyrometallurgical or

hydrometallurgical production methods are exploited to manufacture nickel metal from low-grade minerals. Pyrometallurgical techniques, which involve drying, calcination, reduction, and electric furnace smelting, are suited to treat saprolite to produce a ferronickel or nickel sulfide matte [8]. Some investigations have indicated that the appropriate additives added to laterite ore could improve the separation effect [9–11]; however, this process results in high energy consumption, serious pollution, and reduction of the ferronickel grade of the ores and products. For these reasons, this technique has not been applied in industry yet. Onodera, Agatzini-Leonardou, and others have studied beneficiation methods for laterite ore [12–13]. The results revealed that the consumption of acid caused the decrease of recovery rate of nickel. Hydrometallurgical processes, including high pressure acid leaching (HPAL), atmospheric acid leaching, and ammonia-ammonium carbonate leaching [14], are more appropriate for treating limonite ore that has high iron content but low garnierite content. Ruan *et al.* [15] employed the reduction roasting, ammonia leaching, ex-

Corresponding author: Run-zao Liu E-mail: liurunzao@metall.ustb.edu.cn

© University of Science and Technology Beijing and Springer-Verlag Berlin Heidelberg 2014

tracting, and bioleaching to extract nickel, cobalt, and iron from low-grade nickel laterite ore. The leaching rate of nickel and cobalt were 89.33% and 62.47%, respectively; thus, the recovery rate of cobalt was too low. Ammonia leaching techniques are well suited for treating saprolite, in which the cobalt and iron content are low. The River and Mountains Smelter of Nippon Yakim in Japan applied the reduction roasting and magnetic separation to get ferronickel products; the specific process included grinding for minerals, briquetting with coal, roasting pellets, and magnetic separation [16].

At present, the pyrometallurgical techniques of nickel laterite ore mainly involve adding some coke and coal powders into ores to reduce nickel and iron oxide by high temperature roasting and then using the beneficiation methods to enrich metallic nickel and iron. In recent years, it is found that the ultrafine mineral materials have better reactivity by our research team. The reduction dynamics of ultrafine mineral powders greatly improves by using hydrogen or carbon monoxide as a reductant at a non-melt temperature, and this process can obtain high-grade reduction products. Our team named this oxide reduction scale effect as fine particle reduction [17]. In this paper, H₂ and CO were used as the reductants under high temperature and airtight conditions to reduce nickel laterite ore, and the nickeliferous concentrations were then enriched by magnetic separation. The entire process had a lower energy consumption and a less pollution than the comparable methods, which could provide the material basis for the production smelting of ferro-nickel or nickel alloys.

2. Experimental

2.1. Materials

Nickel laterite ore studied in this paper came from Indonesia. Hydrogen with a purity of greater than 99.99% was employed as a gaseous reductant. To obtain a high reducing atmosphere, semi-coke was put into the reforming furnace to reform the blast furnace gas. This process mainly produces the following chemical reaction:



where ΔG^\ominus is the standard Gibbs free energy (J·mol⁻¹), and T is the temperature (K).

Table 1 shows gas composition in the blast furnace before and after reforming. In Table 1, the CO content of the blast-furnace gas increases to 48.85vol% after reforming, while the corresponding CO₂ content decreases to 1.44vol%. According to calculation, $\alpha(\text{CO})$ reaches 97.14vol% and in-

creases by approximately 38.39vol% after reforming. The reducibility of the blast-furnace gas is obviously elevated after reforming. In this paper, the reduction process using reforming gas as a reductant was referred as CO reduction.

Table 1. Gas composition in the blast furnace before and after reforming

| Composition | H ₂ | O ₂ | N ₂ | CO | CO ₂ | $\alpha(\text{CO})$ |
|------------------|----------------|----------------|----------------|-------|-----------------|---------------------|
| Before reforming | 2.73 | 0.12 | 52.40 | 26.29 | 18.46 | 58.75 |
| After reforming | 4.62 | 0.03 | 44.76 | 48.85 | 1.44 | 97.14 |

Note: $\alpha(\text{CO}) = V(\text{CO}) / [V(\text{CO}) + V(\text{CO}_2)]$, where $\alpha(\text{CO})$ represents the reducibility of reformed gas, $V(\text{CO})$ the CO volume of reformed gas, and $V(\text{CO}_2)$ the CO₂ volume of reformed gas.

2.2. Characterization

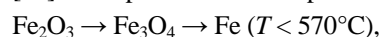
The main chemical composition of the nickel laterite ore was analyzed by atomic absorption spectrometry (AAS) and sequential X-ray fluorescence spectrometry (XRF). X-ray diffraction (XRD) were performed with Cu K_α radiation (50 kV, 200 mA) at a scanning rate of 5°/min from 10° to 90°. A laser particle size analyzer was used to detect the particle size distribution of raw materials. Thermogravimetric-differential thermal analysis (TG-DTA) was conducted under a N₂ atmosphere (flow rate: 100 mL/min, heating rate: 5°C/min).

2.3. Reduction process

The nickel laterite ore contains a large amount of absorbed and crystallized water. Thus, the ore was first dried at 100°C for 10 h in a dryer oven and then crushed using a roll crusher. The crushed materials were sieved by a 100 mesh screen. Because CO reduction was better than H₂ reduction, the reduction products of CO reduction were magnetically separated. The experimental process is shown in Fig. 1.

2.3.1. Thermodynamic analysis

The reduction of the nickel laterite ore can produce some valuable metallic oxides, such as nickel and iron oxides, which can be reduced into metal or protoxide. The nickel oxide reduction process does not generate intermediate oxides, but directly turns NiO into Ni. For iron oxide, however, different products are generated at different temperatures [18]. The specific reduction process is as



The reduction of iron oxide has different reactions in different stages. The corresponding ΔG^\ominus values are shown in Table 2.

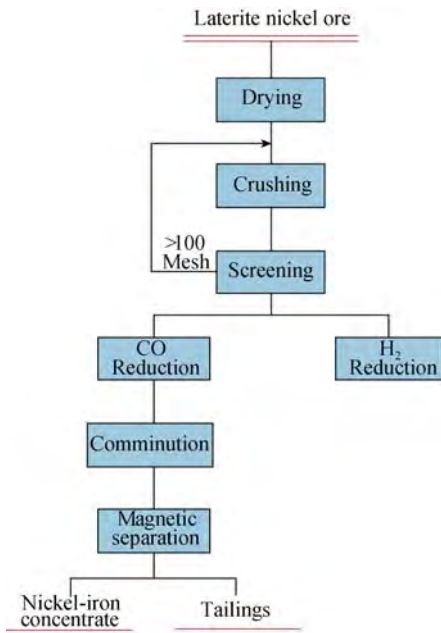


Fig. 1. Flow diagram of the experiment.

Table 2. ΔG^\ominus values for reducing iron and nickel oxides by H_2 or CO

| Reaction | $\Delta G^\ominus = A + BT, J \cdot mol^{-1}$ |
|------------------------------------|---|
| $NiO + H_2 = Ni + H_2O$ | $\Delta G^\ominus = -10104 - 32.40T$ |
| $NiO + CO = Ni + CO_2$ | $\Delta G^\ominus = -46719 + 0.43T$ |
| $3Fe_2O_3 + H_2 = 2Fe_3O_4 + H_2O$ | $\Delta G^\ominus = -15547 - 74.40T$ |
| $3Fe_2O_3 + CO = 2Fe_3O_4 + CO_2$ | $\Delta G^\ominus = -52131 - 41.00T$ |
| $Fe_3O_4 + H_2 = 3FeO + H_2O$ | $\Delta G^\ominus = 71940 - 73.62T$ |
| $Fe_3O_4 + CO = 3FeO + CO_2$ | $\Delta G^\ominus = 35380 - 40.16T$ |
| $Fe_3O_4 + 4H_2 = 3Fe + 4H_2O$ | $\Delta G^\ominus = 142200 - 121.60T$ |
| $Fe_3O_4 + 4CO = 3Fe + 4CO_2$ | $\Delta G^\ominus = -39328 + 34.32T$ |
| $FeO + H_2 = Fe + H_2O$ | $\Delta G^\ominus = 23430 - 16.16T$ |
| $FeO + CO = Fe + CO_2$ | $\Delta G^\ominus = -22800 + 24.26T$ |

Mohamed [19] pointed out that iron and nickel oxides

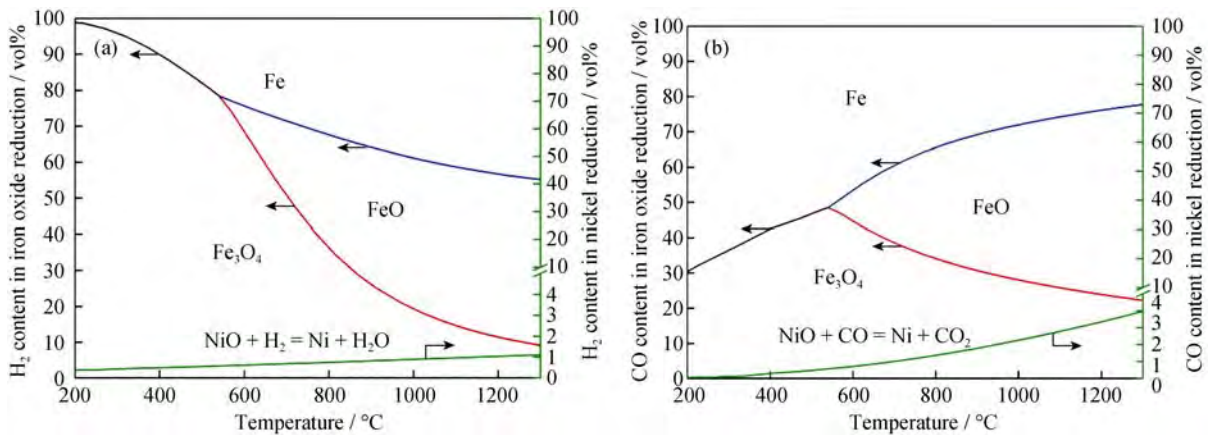


Fig. 2. Thermodynamics of hydrogen reduction (a) and carbon monoxide reduction (b).

could not be directly reduced step-by-step during the actual experimental process. NiO and Fe_2O_3 could be combined to generate $NiFe_2O_4$. In fact, the production of $NiFe_2O_4$ is more conducive for reduction.

The actual Gibbs free energy in the reduction process is $\Delta G = \Delta G^\ominus + RT \ln K$, where K represents the entropy of pressure or activity, and R the molar gas constant, $8.314 J \cdot mol^{-1} \cdot K^{-1}$. When the reaction reaches equilibrium, $\Delta G = 0$ and thus $\Delta G^\ominus = -RT \ln K$. The curve of reaction temperature vs. gas concentration can be obtained through the actual partial pressure of product gases.

Fig. 2 shows the relationship between gas concentration and reaction temperature using H_2 or CO as a reductant to reduce NiO or Fe_xO_y . From the thermodynamic point of view, NiO can be reduced at a lower H_2 (CO) concentration and a lower temperature, while the iron oxide is divided into Fe, FeO, and Fe_3O_4 stable regions; and the iron oxide will produce different products under different temperatures and reduction atmospheres.

2.3.2. Reduction process by hydrogen

According to characterization of raw materials, a fixed-bed fine particle reduction apparatus was designed as shown in Fig. 3. The apparatus mainly includes (a) nitrogen, (b) hydrogen, (c) flowmeter, (d) mixing chamber, (e) horizontal resistance furnace, and (f) control cabinet. The experimental process for the laterite ore reduction is as follows: (1) accurately add 10.0 g of the laterite ore sample into the crucible and put the crucible into the tube furnace; (2) turn on the nitrogen valve (flow rate of 1 L/min) until the furnace temperature reaches the target temperature; (3) suspend the nitrogen flow and, at the same time, turn on the hydrogen valve (flow rate of 0.5 L/min) to start the reduction process; (4) when the reduction process is completed, turn off hydrogen, and turn on nitrogen (flow rate of 1 L/min) again to let the hot reduced sample cool down to room temperature.

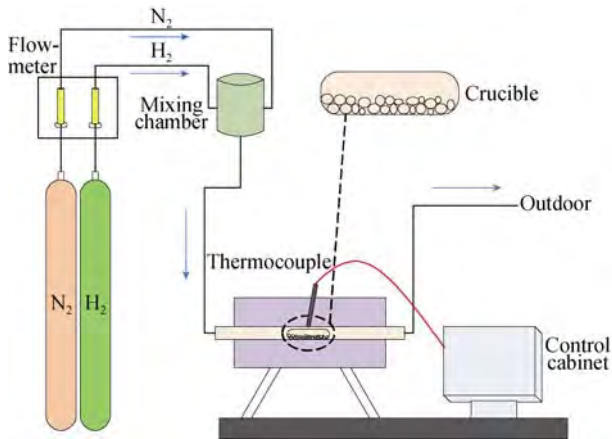


Fig. 3. Schematic diagram of the hydrogen reduction apparatus.

2.3.3. Reduction process by carbon monoxide

To ensure the reduction atmosphere meet experimental requirements, the blast furnace gas was reformed before the reduction process. The diagram of a moving-bed apparatus is shown in Fig. 4.

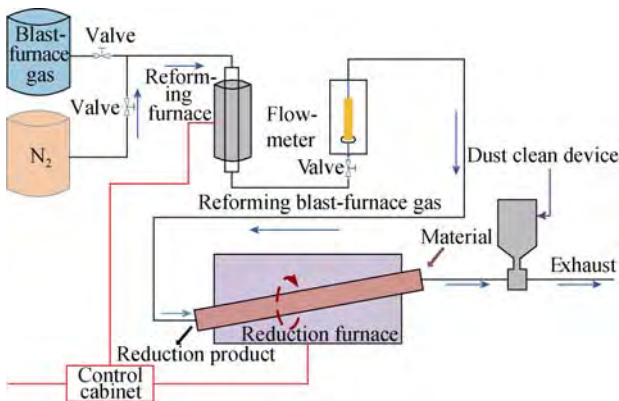


Fig. 4. Schematic diagram of the carbon monoxide apparatus.

The apparatus mainly includes (a) blast-furnace gas, (b) nitrogen, (c) reforming furnace, (d) flowmeter, (e) reduction furnace, (f) control cabinet, and (g) dust clean device. The reduction process used a mixed gaseous reductant, including CO, CO₂, and a trace amount of H₂, which were metered into the reactor. The reduction procedure involved putting semi-coke into the reforming furnace, adjusting the furnace inclination to 1° at 2.5 r/min (the corresponding reduction time is 2 h), and flushing the tube with nitrogen prior to heating. Reducing gases (flow rate of 1.5 m³/h) were then metered into the tube while it was heated to the target temperature. At the same time, the materials were fed from the furnace feeding mouth to begin the reduction reaction. Once the reduction was complete, nitrogen (flow rate of 1.0 m³/h) was metered into the reactor for cooling and protecting.

2.4. Magnetic separation

To obtain higher-grade ferronickel concentrates, the samples were ground in a prototype vibration mill for 10 min and separated using a SLon-100 cycle pulsating magnetic separator (1.2 T) with a working electrical current of 380 A (magnetic field intensity of 0.5 T).

3. Results and discussion

3.1. Characterization of raw laterite ore

The chemical composition of the raw nickel laterite ore is shown in Table 3. The material contains approximately 1.91wt% Ni, 22.50wt% total Fe, 26.48wt% MgO, and 19.50wt% SiO₂, which is typical of a high magnesium saprolite ore.

XRD analysis in Fig. 5 reveals that crystalline phases in the raw materials are mainly consisted of hematite [Fe₂O₃], quartz [SiO₂], serpentine [Mg₃Si₂O₅(OH)₄], hortonolite [(MgFe)₃Si₂O₅(OH)₄], and goethite [FeOOH]. Together with these major phases, a small quantity of kaolin [Al₂Si₂O₅(OH)₄] is observed.

Table 3. Major chemical components of nickel laterite ore

| wt% | | | | | | | | |
|----------------|------|-------|------------------|--------------------------------|------|--------------------------------|------|------------------|
| Total Fe (TFe) | Ni | MgO | SiO ₂ | Al ₂ O ₃ | CaO | Cr ₂ O ₃ | S | Loss on ignition |
| 22.50 | 1.91 | 26.48 | 19.50 | 2.40 | 0.93 | 0.82 | 0.06 | 13.58 |

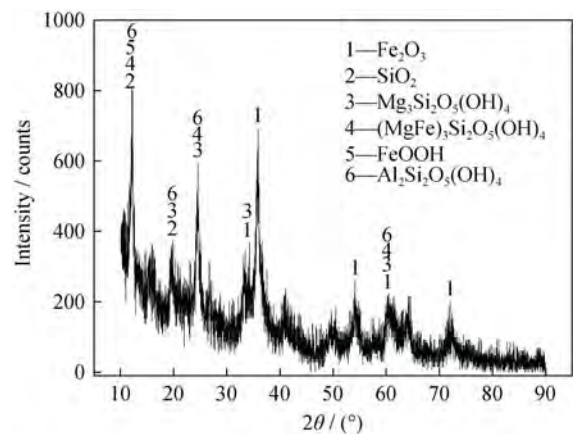


Fig. 5. XRD patterns of nickel laterite ore.

Fig. 6 reveals that the granularity of the raw materials mainly ranges from 0.3–20 μm. The particle size distribution is similarly concentrated. The average particle size of the raw materials is 3 μm, which belongs to the ultrafine grain dust category and meets requirements for the fine particle reduction.

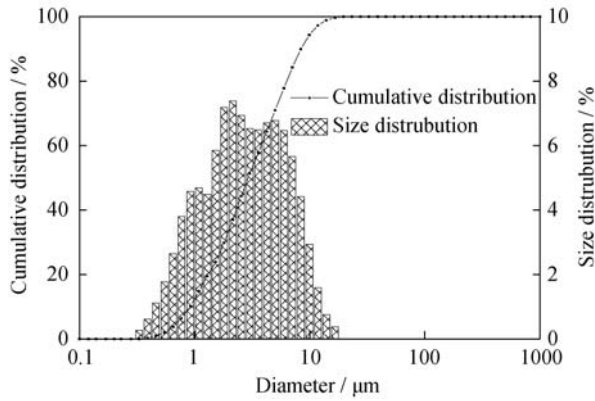


Fig. 6. Particle size distribution of the raw materials.

The TG–DTA curves showing the thermal properties of the laterite ore are presented in Fig. 7. The weight loss (Δm) process can be divided into four steps: (1) the TG curve declines due to free water evaporation in the primary stage, corresponding to a weight loss of 1.45%; (2) the endothermic DTA peak at 289°C is accompanied by a decline in the TG curve, corresponding to crystallization water removal of serpentine, goethite, and other complex compounds [20]; (3) the endothermic peak centered at 657°C is caused by dehydroxylation of lizardite [21]; and (4) the exothermic peak at 841°C, which results from recrystallization of forsterite, does not have any associated weight loss. The dehydration process can be expressed by the following equations:

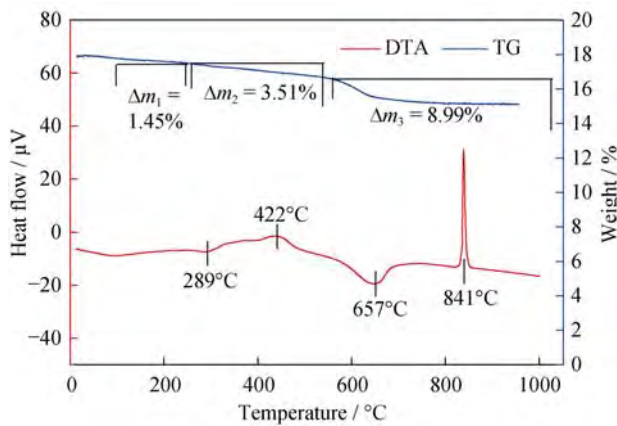
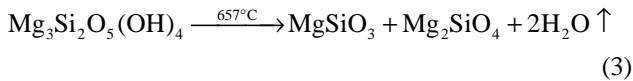
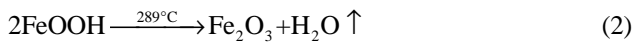


Fig. 7. TG-DTA curves of the nickel laterite ore.

3.2. Hydrogen reduction

The relationship between temperature and the grade of TFe and Ni in hydrogen reduction is shown in Fig. 8. When the temperature rises from 700°C to 1000°C, the total iron content (TFe) increases from 25.25wt% to approximately

34.95wt%, and the corresponding nickel content increases from 3.13wt% to 3.98wt%. This result shows that the nickel laterite ore can be reduced by hydrogen, which also enriches nickel and iron in the raw materials. Raising the temperature can increase the nickel and iron grades in the product; however, the temperature should not be too high, considering the energy consumption of the reduction process and the sintering of the reduction products at 1000°C.

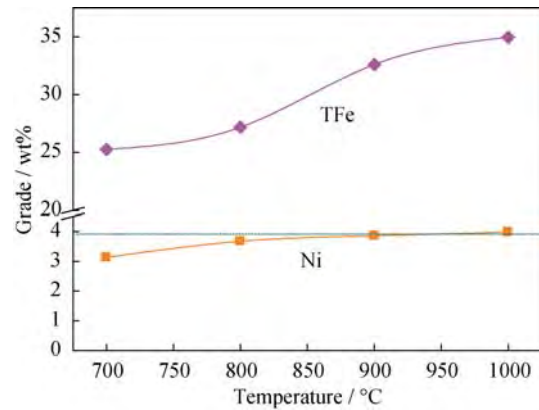


Fig. 8. Effect of reduction temperature on nickel-iron beneficiation during hydrogen reduction (reduced for 2 h).

From the above discussion, the hydrogen reduction effect was not significant, and the result was explained by the presence of an isomorphism in the ore due to the replacement of magnesium by nickel and iron [22]. To achieve nickel and iron beneficiation, the structures of goethite and hortonolite must be destroyed. In addition, a dynamic study showed that the reactive mode was determined by reduction temperature, while the controlling steps at the initial, middle, and later stages were chemical reaction-, mixed-, and diffusion-controlled, respectively [23].

The XRD pattern of the reduced nickel laterite ore is shown in Fig. 9. According to this diffraction pattern, a series of FeNi and Fe are generated in the product, and parts of forsterite [Mg_2SiO_4] and fayalite [Fe_2SiO_4] are found. The most important feature of this result is the transformation of magnesium hydrosilicate to the forsterite phase in the reduced product.

3.3. Carbon monoxide reduction

Fig. 10 shows the grades of TFe and Ni as a function of reduction temperature. With increasing reduction temperature, the TFe grade initially falls but exhibits a rising trend overall. When the temperature rises from 700°C to 1000°C, the nickel content increases from 3.07wt% to approximately 4.47wt%, and the corresponding iron content increases from 39.53wt% to 50.61wt%. The experimental results demon-

strate that a higher temperature promotes higher nickel and iron contents. This is attributed to the fact that increasing the temperature improves the degree of metallization of both iron and nickel and also liberates more nickel and iron-liberated silicates.

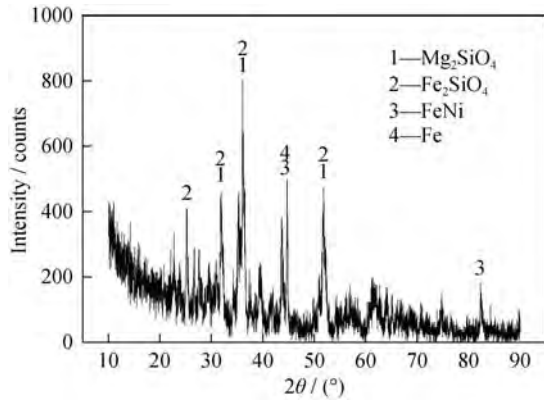


Fig. 9. XRD pattern of the reduction product at 1000°C by hydrogen reduction.

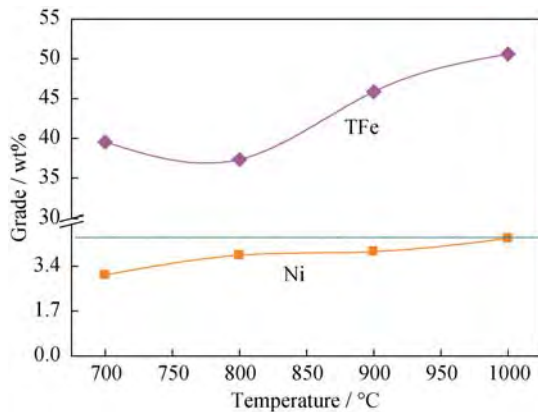


Fig. 10. Effect of reduction temperature on nickel-iron beneficiation (reduced for 2 h) during carbon monoxide reduction.

Fig. 11 shows the crystalline phase of the reductive product analyzed by XRD. A series of forsterite [Mg_2SiO_4] and fayalite [Fe_2SiO_4] are generated in the product, and parts of metallic Ni and metallic Fe are also found. Combining the results of Fig. 7 and Fig. 11, it can be concluded that high temperature promotes the crystalline phase structure transition of laterite ore.

Comparing the reduction results of H_2 and CO , it is obvious that the CO reductive effect is better than H_2 for the improvement of nickel and iron grades. According to the shrinking unreacted core model, the gaseous reduction of the laterite ore is a complex multi-phase gas–solid reaction consisting of three steps: external diffusion, internal diffusion, and interfacial chemical reaction. Carbon monoxide is able to accelerate the surface reaction rate, and the favorable

dynamic condition is conducive to mass transfer and gaseous diffusion.

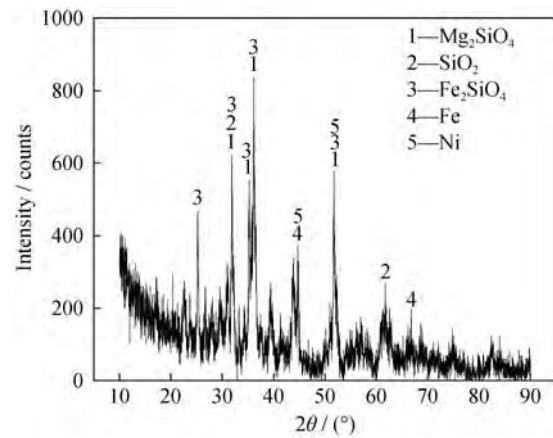


Fig. 11. XRD pattern of the reduction product at 1000°C by carbon monoxide reduction.

3.4. Magnetic separation

Magnetic separation was carried out on the reduced ores at different reduction temperatures ranging from 700°C to 1000°C; the results are shown in Fig. 12. When the temperature is maintained at 700°C, the recovery rates of iron and nickel are fairly low even though the nickel content is approximately 3.57wt%; the iron and nickel recoveries are 40.75% and 45.23%, respectively, indicating a very low production rate.

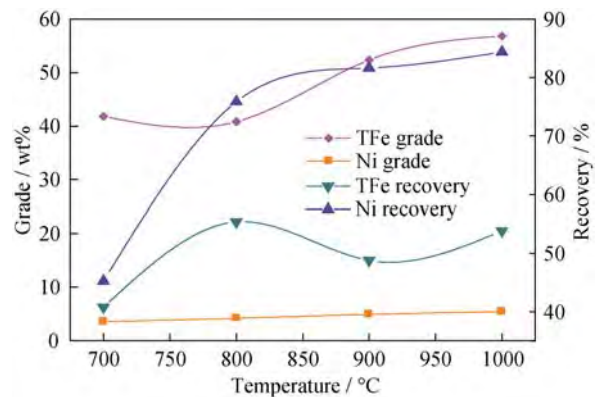


Fig. 12. Effect of reduction temperature on nickel-iron beneficiation during magnetic separation.

By further increasing the reduction temperature to 1000°C, the metallization ratio of total iron increases, and the recovery rates of both iron and nickel increases rapidly, with the maximum recoveries of 53.76% and 84.38%, respectively. In addition, the nickel content increases from 3.57wt% to 5.43wt%. Fig. 12 shows the similar trend as those in Figs. 8 and 10, this is, increasing the temperature

results in the enhanced nickel content and recovery rate. The results indicate that the physical separation method affects the concentrations of nickel and iron, and a higher temperature can enhance the crystalline phase structure transition of the laterite ore and promote the reduction rate of nickel and iron oxides.

4. Conclusions

(1) Fine particle reduction and magnetic separation were conducted on the nickel laterite ore. The results indicate that a higher temperature can enhance the crystalline phase structure transition of the nickel laterite ore and increase the reduction rate. Considering the energy consumption of the reduction process and the sintering phenomenon of reduction products at 1000°C, however, the reduction temperature should not be too high.

(2) The nickel and iron grades can be improved in the reduction process. However, because nickel and iron replace magnesium as an isomorphism in the ore, the reduction effects are not ideal, and the reductive products require further nickel and iron enrichment by physical separation. After magnetic separation, the maximum nickel and total iron contents of the concentrates are 5.43wt% and 56.86wt%, with the corresponding recovery rates of 84.38% and 53.76%, respectively. The results show that nickel and iron can be enriched by magnetic separation, but the iron recovery rate is not high.

Acknowledgements

The authors are grateful for the support by Tangshan Iron & Steel Co. Ltd., China.

References

- [1] G.G. Charles, *Mineral Commodity Summaries*, United States Geological Survey, Virginia, 2003, p. 14.
- [2] T. Norgate and S. Jahanshahi, Low grade ores: smelt, leach or concentrate, *Miner. Eng.*, 23(2010), p. 65.
- [3] C.T. Harris, J.G. Peacey, and C.A. Pickles, Selective sulphidation of a nickeliferous lateritic ore, *Miner. Eng.*, 24(2011), p. 657.
- [4] T. Norgate and S. Jahanshahi, Assessing the energy and greenhouse gas footprints of nickel laterite processing, *Miner. Eng.*, 24(2010), p. 698.
- [5] J.H. Zhu, Exploration laterite-nickel ore and analysis on utilization technology, *World Nonferrous Met.*, 10(2007), p. 7.
- [6] Y. Liu and Z.F. Cong, Atmospheric sulphuric acid leaching of saprolitic nickel laterites, *Nonferrous Min. Metall.*, 24(2008), No. 2, p. 34.
- [7] J.H. Li, W. Chen, and Z.H. Xiao, Review on process technologies of laterite-nickel ore, *Hydrometall. China*, 23(2004), No. 4, p. 191.
- [8] B. Li, H. Wang, and Y.G. Wei, The reduction of nickel from low-grade nickel laterite ore using a solid-state deoxidization method, *Miner. Eng.*, 24(2011), p. 1556.
- [9] G.H. Li, M.J. Rao, T. Jiang, Q.Q. Huang, T.M. Shi, and Y.B. Zhang, Innovative process for preparing ferronickel materials from laterite ore by reduction roasting-magnetic separation, *Chin. J. Nonferrous Met.*, 21(2011), No. 12, p. 3137.
- [10] M. Jiang, T.C. Sun, Z.G. Liu, J. Kou, N. Liu, and S.Y. Zhang, Mechanism of sodium sulfate in promoting selective reduction of nickel laterite ore during reduction roasting process, *Int. J. Miner. Process.*, 123(2013), p. 32.
- [11] W. Liang, H. Wang, J.G. Fu, and Z.X. He, High recovery of ferro-nickel from low grade nickel laterite ore, *J. Cent. South Univ. Sci. Technol.*, 42(2011), No. 8, p. 2173.
- [12] J. Onodera, T. Inoue, and T. Imaizumi, Attempts at the beneficiation of laterite nickel ore, *Int. J. Miner. Process.*, 19(1987), p. 25.
- [13] S. Agatzini-Leonardou, I.G. Zafiratos, and D. Spathis, Beneficiation of a Greek serpentinitic nickeliferous ore: Part I. Mineral processing, *Hydrometallurgy*, 74(2004), p. 259.
- [14] B.K. Loveday, The use of oxygen in high pressure acid leaching of nickel laterites, *Miner. Eng.*, 21(2008), p. 533.
- [15] S.F. Ruan, P.H. Jiang, C.Y. Wang, F. Yin, and Y.Q. Chen, Experimental study on low grade nickeliferous laterite ore with selective reduction roasting technology, *Min. Metall.*, 16(2007), No. 2, p. 31.
- [16] J. Kim, D. Dodbibba, H. Tanno, K. Okaya, S. Matsuo, and T. Fujita, Calcination of low-grade laterite for concentration of Ni by magnetic separation, *Miner. Eng.*, 23(2010), p. 282.
- [17] P.Y. Chen, J.T. Gao, S.Q. Li, Y.T. Zhang, R.Z. Liu, and J.L. Zhang, A new technic experimental study on precise reduction of iron oxide-separation of non-molten of iron oxide, *J. Sichuan Univ. Eng. Sci. Ed.*, 43(2011), No. 5, p. 195.
- [18] X.H. Huang, *Theory of Ferrous Metallurgy*, Metallurgy Industry Press, Beijing, 2010, p. 285.
- [19] H.K. Mohamed, Isothermal reduction kinetics at 900-1100°C of NiFe₂O₄ sintered at 1000-1200°C, *J. Anal. Appl. Pyrol.*, 73(2005), p. 123.
- [20] J.H. Li, X.H. Li, Q.Y. Hu, Z.X. Wang, Y.Y. Zhou, J.C. Zheng, W.R. Liu, and L.J. Li, Effect of pre-roasting on leaching of laterite, *Hydrometallurgy*, 99(2009), p. 84.
- [21] J. Lu, S.J. Liu, J.S. Guan, W.G. Du, F. Pan, and S. Yang, The effect of sodium sulphate on the hydrogen reduction process of nickel laterite ore, *Miner. Eng.*, 49(2013), p. 154.
- [22] C.A. Pickles, C.T. Harris, J. Peacey, and J. Forster, Thermodynamic analysis of the Fe-Ni-Co-Mg-Si-O-H-S-C-Cl system for selective sulphidation of a nickeliferous limonitic laterite ore, *Miner. Eng.*, 54(2013), p. 52.
- [23] Z.K. Li, X.Z. Yuan, and C.C. Lin, A simulation study on the pre-reduction and calcination process of laterite ore in rotary kiln, *Ferro-alloys*, 40(2009), p. 24.